Check for updates

Angewandte Chemie International Edition

Angewandte International Edition Chemie

How to cite: *Angew. Chem. Int. Ed.* **2026**, e8019368
doi.org/10.1002/anie.8019368

COMMUNICATION OPEN ACCESS

A Homoleptic Biradicaloid-Ligated Analogue of Ferrocene

David Zuber[1] | Robert Kruk[2] | Oksana Storcheva[1] | Michael Neuwirt[1] | Peter Coburger[1] | Oliver P. E. Townrow[2]

[1]Chemistry Department, Technical University of Munich, TUM School of Natural Sciences, Garching, Germany | [2]Institute of Nanotechnology, Karlsruhe Institute of Technology, Karlsruhe, Germany

Correspondence: Peter Coburger (peter.coburger@tum.de) | Oliver P. E. Townrow (oliver.townrow@kit.edu)

Received: 15 July 2026 | **Revised:** 13 October 2026 | **Accepted:** 2 November 2026

Keywords: biradicaloids | iron | organometallics | sandwich complexes

ABSTRACT

In this communication, we report the synthesis, characterisation and electronic structure of a ferrocene analogue containing two biradicaloid ligands, representing the first homoleptic sandwich complex in this ligand class. In this quest, we found that the target compound was unattainable via routes involving Fe(0) or Fe(II) intermediates, and counterintuitively that the rare and much less-explored +1 oxidation state was crucial for the synthesis.

1 | Introduction

Ferrocenes are arguably the archetypal organometallic sandwich complex class, with a vast range of applications across the chemical and physical sciences [1]. Their intense study is owed to the highly customisable cyclopentadienyl rings which flank the ferrous centre, altering the properties of the complex [2–6]. These structure–property relationships have intrigued generations of chemists, leading to libraries of such derivatives, all with their own reactivity profiles and physical properties.

Closed-shell phosphacyclic biradicaloids have recently entered the limelight as a new class of heterocyclic compounds with intriguing electronic properties [7–17]. Their electronic structures feature two spatially separated radical centres and consequentially, they have been employed in a variety of unusual bond-activation reactions [18–25]. Simultaneously, the radicals are incorporated within a partially delocalized 6π-electron system, suggesting that they should also be capable of stabilizing transition-metal centres through π-coordination, a concept first realized by Grützmacher and co-workers in 2020 [26]. Since then, a range of complexes of several transition metals and main group elements have been reported, highlighting the versatility of phosphacyclic biradicaloids as supporting ligands [23, 25, 27, 28]. Increasing the ring size to five (LC_3P_2), we developed the phosphonium-substituted diphosphaindenylide **PPI**, a phosphorus-rich analogue of the indenyl anion in which two carbon atoms of the five-membered ring are replaced by phosphorus. Like $L_2C_2P_2$, **PPI** features significant contributions from biradicaloid resonance forms featuring spatially separated spin centres at the phosphorus atoms. The ability for **PPI** to act as a π–ligand has recently been demonstrated on a series of chromium and iron carbonyl complexes (Figure 1) [16, 29]. Importantly to this study, all known examples of complexes containing $L_2C_2P_2$ and PPI to date feature a half-sandwich structure.

2 | Results and Discussion

With the goal of synthesising a homoleptic sandwich complex with this ligand class, we chose to first target a ferrocene analogue (Scheme 1). To keep valence isoelectronic to ferrocene, one requires 18-VE dicationic complex with **PPI**, that is $[Fe(\eta^5\text{-}\mathbf{PPI})_2]^{2+}$. We attempted to coordinate **PPI** to $[FeCl_2]$, like in the formation of the aforementioned $[NiBr_2(\eta^4\text{-}IPr_2C_2P_2)]$ (IPr = 1,3-bis(2,6-diisopropylphenyl)imidazol-2-ylidene) complex, which resulted in no reaction, even in combination with sodium

This is an open access article under the terms of the Creative Commons Attribution License, which permits use, distribution and reproduction in any medium, provided the original work is properly cited.
© 2026 The Author(s). *Angewandte Chemie International Edition* published by Wiley-VCH GmbH

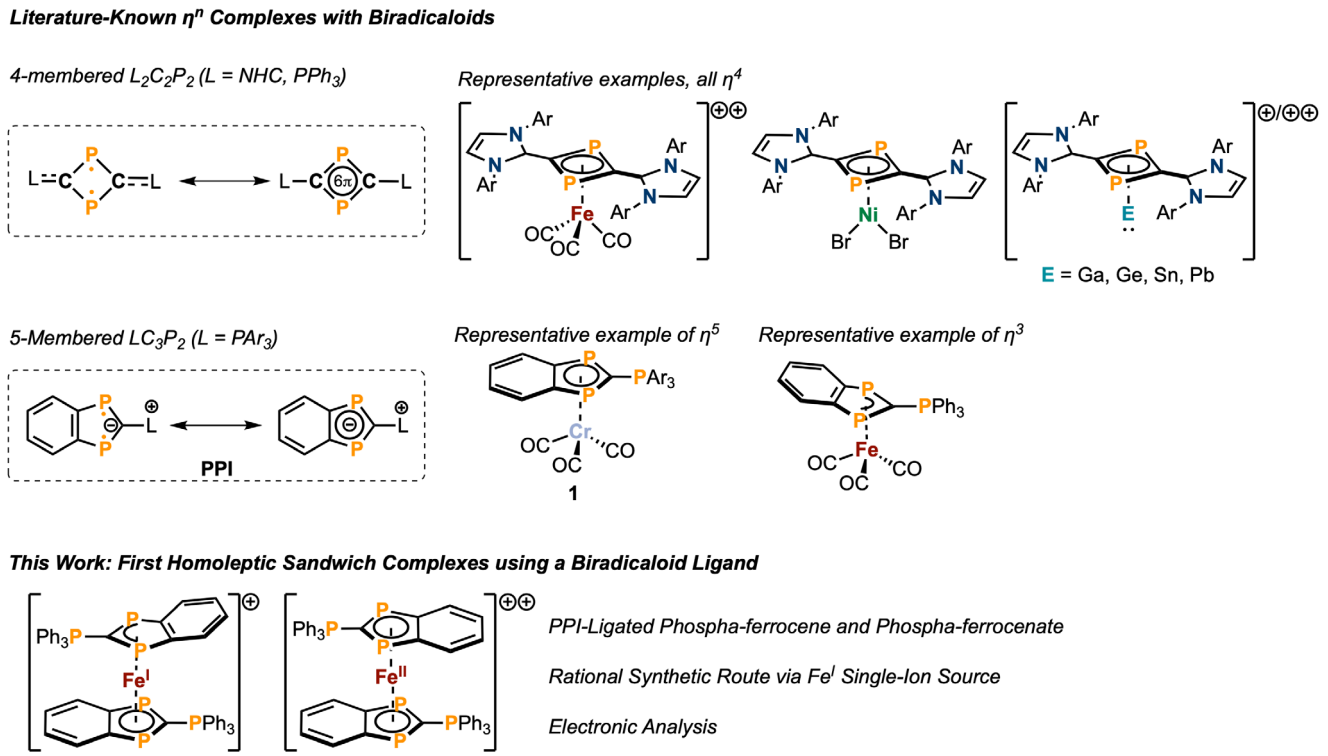


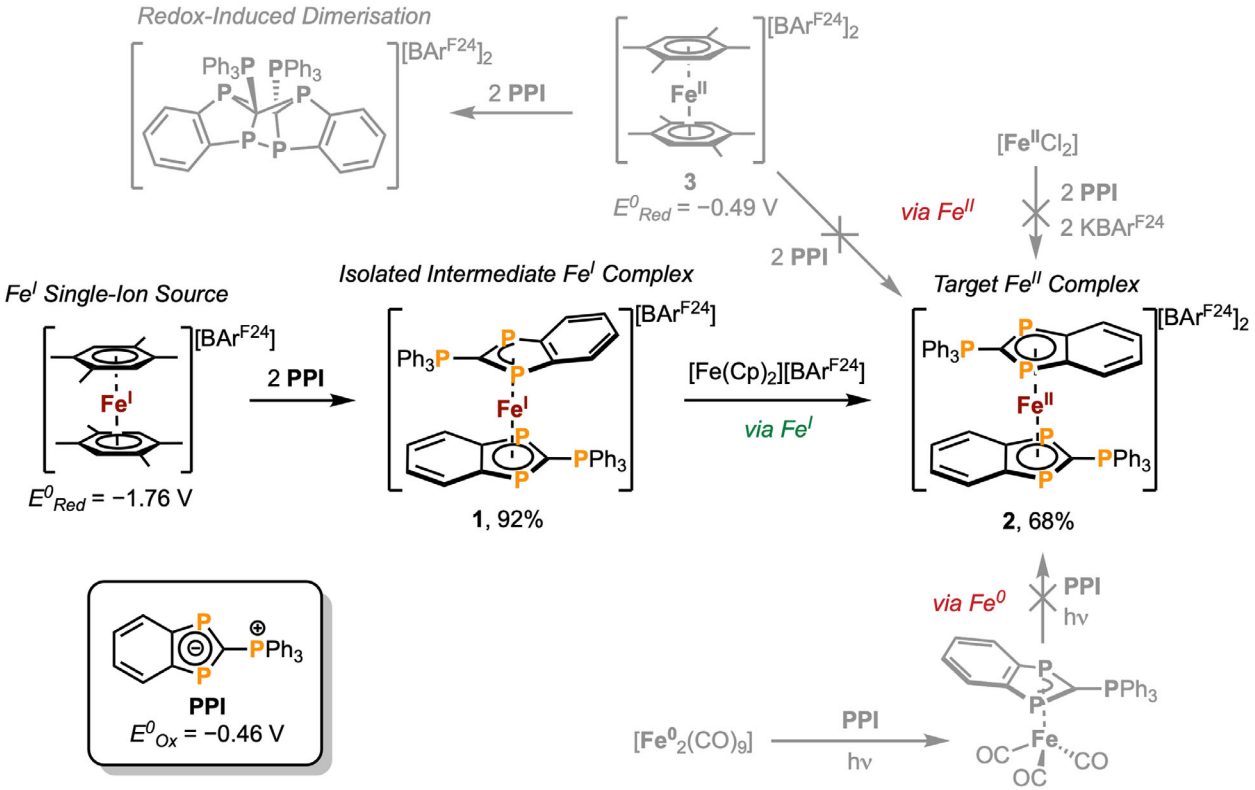
FIGURE 1 | Selected literature examples of biradicaloid-ligated complexes and contextualisation.

tetrakis(3,5-bis(trifluoromethyl)phenyl)borate ($NaBAr^{F24}$). To mitigate solubility effects, we then tried the iron(II) sandwich complex $[Fe(Dur)_2][BAr^{F24}]_2$ (**3**, Dur = 1,2,4,5-tetramethylbenzene), featuring a soluble source of iron(II) and two weakly-coordinating BAr^{F24} ions. This resulted in redox-induced dimerisation of the **PPI** ligand as observed previously for reactions with $[Fe(Cp)_2][BF_4]$, owing to an anodic reduction potential for **3** at (E^0_{red} = −0.49 V vs. $Fc^{0/+}$) [30], which is very close to the formal oxidation potential of **PPI** (E^0_{ox} = −0.46 V vs. $Fc^{0/+}$) [30]. Previous attempts at forming an iron(0) complex with **PPI** resulted in a half-sandwich complex, $[Fe(CO)_3(\eta^3\text{-}\mathbf{PPI})]$ [31]. It was therefore obvious that one must choose the iron source carefully, so that its redox potential is compatible with **PPI**. This led us to design a strategy using our recently reported complex $[Fe(\eta^6\text{-}Dur)_2][BAr^{F24}]$, which we showed to be a convenient source of Fe^+ towards various neutrally-charged ligands (pyridines, phosphines, carbenes) [30], and has a compatible redox profile (E^0_{ox} = −0.49 V vs. $Fc^{0/+}$, E^0_{red} = −1.76 V vs. $Fc^{0/+}$) with respect to the redox window of the ligand, *vide supra*. We hypothesised that a subsequent one-electron oxidation of the resultant sandwich complex would then yield our target ferrocene analogue.

Stirring $[Fe(\eta^6\text{-}Dur)_2][BAr^{F24}]$ with **PPI** overnight in fluorobenzene (FB) yielded a brown solution. The solvent was removed, and the crude brown powder containing $[Fe(\eta^3\text{-}\mathbf{PPI})(\eta^5\text{-}\mathbf{PPI})][BAr^{F24}]$ (**1**) was recrystallised from toluene/*n*-hexane (50:1) at −40°C, as red–brown crystals suitable for single crystal x-ray diffraction in a 92% crystalline yield. Complex **1** features two **PPI** ligands, one interacting with the Fe centre in an η^5 fashion like $[Cr(CO)_3(\eta^5\text{-}\mathbf{PPI})]$ [16], and the other in an η^3 fashion like $[Fe(CO)_3(\eta^3\text{-}\mathbf{PPI})]$ [31]. The cationic component of complex **1** was completely silent by NMR spectroscopy, showing only signals related to the BAr^{F24} counterion and residual solvent. Electrospray ionisation mass spectrometry (ESI-MS), however, was more indicative, finding the expected molecular ion peak for the homoleptic sandwich complex at 880.0728 *m*/*z* (*calc.* 880.0743 Da).

Cyclic voltammetry (CV) was performed on complex **1** to see whether the target Fe(II) complex was at least electrochemically accessible. The cyclic voltammogram of complex **1** in 1,2-difluorobenzene shows two quasi-reversible redox events at E_1^0 = −1.41 V and E_2^0 = −0.43 V (all potentials are given relative to the ferrocene/ferrocenium redox couple, $Fc^{0/+}$ = 0) as well as an irreversible event found only at low scan rates, close to solvent oxidation at E_3^{pa} = +1.04 V (Figures 3 and S24). We tentatively assign these as $Fe^{0/I}$, $Fe^{I/II}$ and $Fe^{II/III}$ though ligand-based redox events cannot be excluded and the $Fe^{II/III}$ event is particularly anodic. The $Fe^{0/I}$ event, appears to be accompanied by other events, and its asymmetry increases as a function of scan rate. Chemical reduction with KC_8 resulted only in an intractable mixture. It is also notably rare for ferrocenes to have stable $Fe^{I/II}$ redox couples, with known examples being particularly cathodic [32–36]. Exploiting the electrochemical event at E_2^0 = −0.43 V, an NMR scale reaction with $[Fe(Cp)_2][BAr^{F24}]$ was performed, yielding a brown solution with two resonances in the $^{31}P\{^1H\}$ NMR spectrum at δ = 17.9 ppm (s, br., C_3P_2), and 29.2 ppm (t, $^2J_{PP}$ = 61 Hz, PPh_3), indicating oxidation from paramagnetic Fe(I) to diamagnetic Fe(II). This contrasts with the reaction of free **PPI** with $[Fe(Cp)_2][BAr^{F24}]$, which results in dimerisation, *vide supra*, exemplifying the stability by coordination. Due to the high-yielding synthesis of complex **1**, we developed a one-pot procedure for the scale-up reaction. For this $[Fe(Dur)_2][BAr^{F24}]$ was stirred with **PPI** overnight in FB, yielding a brown solution containing complex **1** and free durene. The solution was cooled to

15213773, 0, Downloaded from https://onlinelibrary.wiley.com/doi/10.1002/anie.80193368 by Karlsruher Institut Fur Technologie, Wiley Online Library on [16/11/2026]. See the Terms and Conditions (https://onlinelibrary.wiley.com/terms-and-conditions) on Wiley Online Library for rules of use; OA articles are governed by the applicable Creative Commons License



SCHEME 1 | Synthetic protocol towards $[Fe(\eta^5\text{-}\mathbf{PPI})_2][BAr^{F24}]_2$ (**2**). Grey pathways show attempted, unsuccessful, syntheses from other oxidation states of iron. Redox potentials were measured using cyclic voltammetry (CV) in 1,2-difluorobenzene (DFB), referenced to the ferrocene/ferrocenium redox couple ($Fc^{0/+} = 0$).

−10°C and $[Fe(Cp)_2][BAr^{F24}]$ was added dropwise before stirring at room temperature overnight, yielding $[Fe(\eta^5\text{-}\mathbf{PPI})_2][BAr^{F24}]_2$ (**2**) in a 68% yield.

Having succeeded in the isolation of our target complexes **1** and **2**, we determined their molecular structures by SCXRD (Figure 2). To compare their structures, we use three diagnostic parameters which we established in an earlier work and their definitions are provided in Section S3 [31]. For complex **2**, the ring-slip parameters r of 0.097 and 0.135 Å, together with the small fold angles φ of 2.8(1)° and 3.0(1)° clearly show the η^5 coordination of both **PPI** ligands to the iron centre. Within experimental uncertainty, the plane distances d are equal (1.6961(9) vs. 1.6996(9) Å). In **1**, r and φ are increased compared to **2**. One **PPI** ligand exhibits $r = 0.388$ Å and $\varphi = 6.5(2)°$, whereas the second displays $r = 0.794$ Å and $\varphi = 19.8(1)°$. The former values still allow for the assignment of an η^5 coordination mode, while the latter are consistent with an η^3 coordination mode. Finally, the plane distances in **2** (1.6961(9) and 1.6996(9) Å) are shorter than the ones found in **1**, where the η^5-coordinated **PPI** ligand adopts a smaller distance to the iron centre than the η^3-coordinated ligand (1.7323(5) vs. 1.7531(5) Å).

Superconducting quantum interference device (SQUID) magnetometry revealed that complex **1** exhibits a doublet magnetic ground state ($S = 1/2$) (Figure S26). Plotting M vs. H/T found that the magnetisation curve does not follow a Brillouin function based on the EPR-derived g-values (Figure S27). Cooling from 8.0 to 1.8 K, we observe increasing discrepancies between the experimental and theoretical spin-only magnetic moment (Table S2), which can be attributed to weak antiferromagnetic inter-

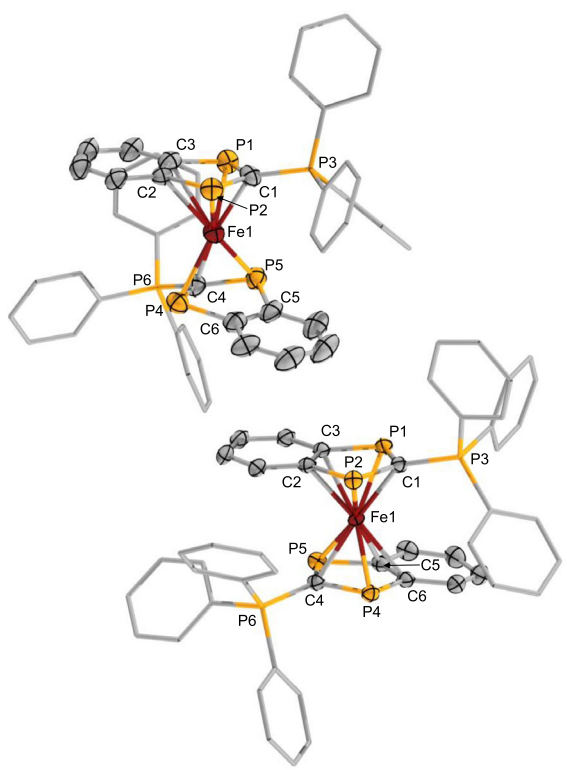


FIGURE 2 | Molecular structures of complexes **1** (top) and **2** (bottom) with ellipsoids at the 50% probability level. Counterions (BAr^{F24}) and hydrogen atoms are omitted, and PPh_3 groups are drawn as wireframes for clarity.

15213773, 0, Downloaded from https://onlinelibrary.wiley.com/doi/10.1002/anie.80193368 by Karlsruher Institut Fur Technologie, Wiley Online Library on [16/11/2026]. See the Terms and Conditions (https://onlinelibrary.wiley.com/terms-and-conditions) on Wiley Online Library for rules of use; OA articles are governed by the applicable Creative Commons License

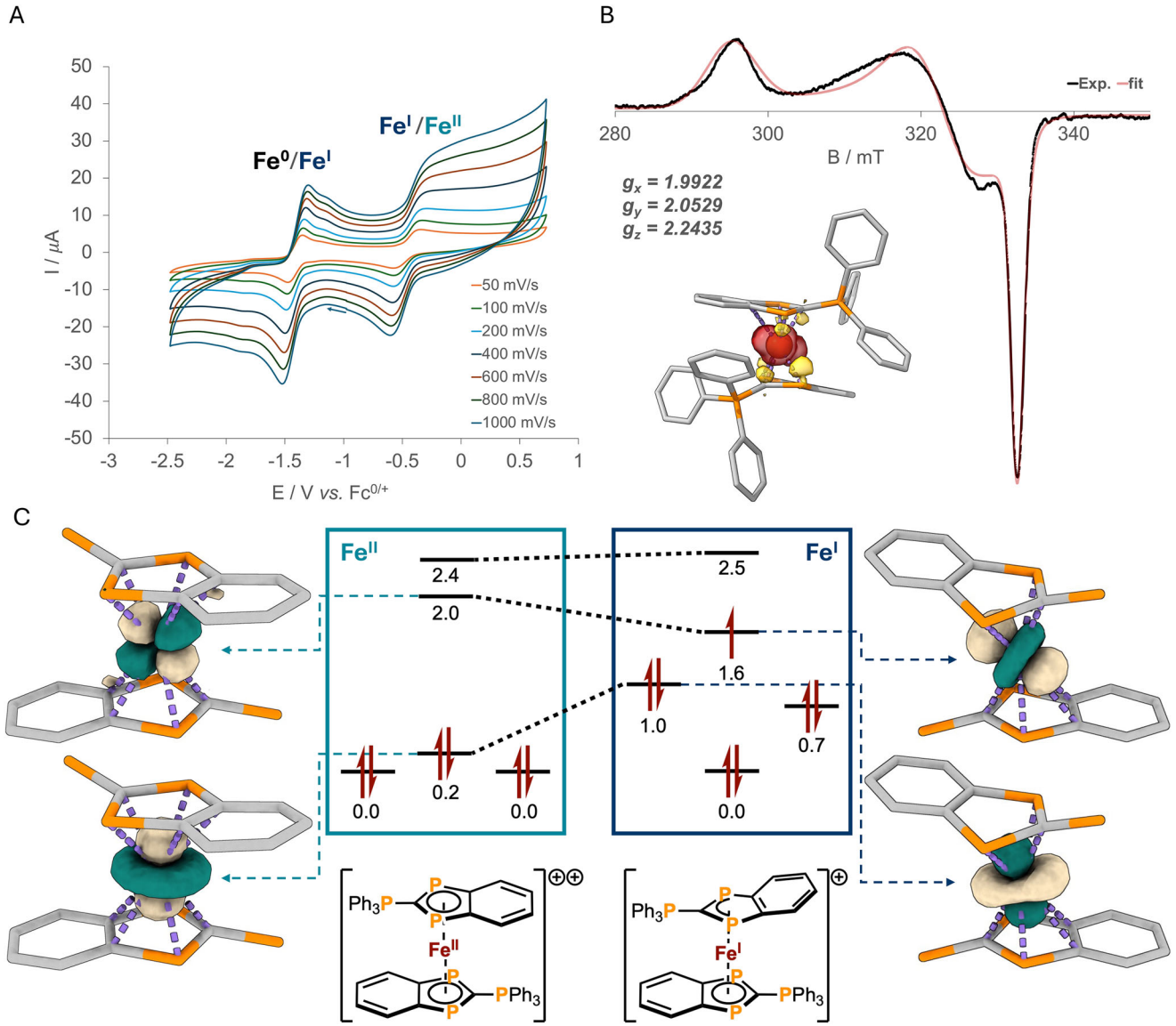


FIGURE 3 | Electronic analysis of complexes **1** and **2**. (A) Cyclic voltammetry of complex **1** (Top: 50–1000 mV s^{-1}; 1.0 mM, 0.1 M $[NBu_4][PF_6]$, 1,2-DFB, room temperature, arrows indicate starting points of the scans and their direction. (B) X-band EPR spectrum of complex **1** (frozen toluene solution at −120°C) together with the fitted spectrum using the given *g* tensor and spin-density plot of **1** obtained from CASSCF(9,9)/def2-TZVP. (C) d-orbital splitting diagrams of **1** and **2** obtained from AILFT calculations at the CASSCF-NEVPT2/def2-SVP level using the ORCA program package [38–40]. Energies given in eV relative to the lowest energy molecular orbital displayed.

actions. More in-depth temperature-dependent analyses were hampered by the presence of nanogram amounts of a ferromagnetic impurity, which we hypothesise to be elemental iron from partial sample disproportionation. In line with the SQUID results, a toluene solution of complex **1** shows a single broad resonance in the x-band EPR spectrum at room temperature, with g_{iso} = 2.1079 (Figure S25). Line-fitting of the spectrum obtained from a frozen toluene sample at −120°C afforded the principal components of the *g*-tensor with g_x = 1.9922, g_y = 2.0529 and g_z = 2.2435 (Figure 3). The comparatively high anisotropy of this rhombic g-tensor indicates the presence of a metal-centred unpaired electron in complex **1**. Indeed, CASSCF-NEVPT2/def2-SVP/def2-TZVP (P)//def2-TZVPP (Fe) calculations qualitatively reproduce the experimental g values (g_x = 2.001, g_y = 2.092, g_z = 2.325) and reveal a $3d^7$ configuration at iron with an iron-centred SONO (singly occupied natural orbital). This SONO shows contributions of 89% of a d-orbital hybrid on Fe, together with minor antibonding contributions from the **PPI** ligands. Occupation of this antibonding orbital in complex **1** rationalises why the experimentally observed contraction of the plane distances when complex **1** is oxidised to complex **2**, *vide supra*. Considering both experimental and computational results, we can safely characterise complex **1** as a low-spin Fe(I) sandwich complex. The low-spin state of **1** is particularly noteworthy, as the related cyclopentadienyl derivative $[Fe(Cp^{ttt})_2]^-$ adopts a high-spin state with S = 3/2 (Cp^{ttt} = 1,2,4-$C_5H_2{}^tBu_3$) [36]. Indeed, CASSCF-NEVPT2 calculations on the Fe(I) bis(cyclopentadienyl) and bis(indenyl) complexes $[Fe(Cp)_2]^-$ and $[Fe(C_9H_7)_2]^-$ show a clear preference for the high-spin state (ΔG_{DQ} = 10.6 and 10.7 kcal•mol^{-1}, respectively). In contrast, the doublet state in **1** lies below the quartet state with ΔG_{DQ} = −6.1 kcal•mol^{-1} (see Supporting Information).

15213773, 0, Downloaded from https://onlinelibrary.wiley.com/doi/10.1002/anie.80193368 by Karlsruher Institut Fur Technologie, Wiley Online Library on [16/11/2026]. See the Terms and Conditions (https://onlinelibrary.wiley.com/terms-and-conditions) on Wiley Online Library for rules of use; OA articles are governed by the applicable Creative Commons License

To gain further insight into the electronic structures of complexes **1** and **2**, ab initio ligand field (AILFT) calculations were performed using the ORCA program package [37, 38]. AILFT enables the extraction of ligand-field splitting patterns from CASSCF wavefunctions (see Supporting Information). For comparison, analogous calculations were carried out for the bis(cyclopentadienyl) and bis(indenyl) complexes.

The low-spin Fe(II) complexes $[Fe(Cp)_2]$, $[Fe(C_9H_7)_2]$, and complex **2** exhibit the characteristic metallocene ligand-field splitting pattern, comprising a set of low-lying, energetically similar d_{xy}, d_{x2-y2} and d_{z2} orbitals and a pair of higher-lying d_{xz} and d_{yz} orbitals (Figure 3) with differences in degeneracy due to the reduced symmetry. More importantly, the d_{xz} and d_{yz} orbitals in complex **2** are substantially stabilized relative to those in ferrocene, being lowered by 1.3 and 0.9 eV, respectively, and by 0.6 and 0.7 eV relative to $[Fe(C_9H_7)_2]$. These results identify **PPI** as a comparatively weak-field ligand towards Fe(II). Upon inspection of the AILFT results for complex **1**, the mixed η^5/η^3 coordination mode of the **PPI** ligands lowers the local symmetry around the iron centre, resulting in substantial mixing of the metal-based d orbitals such that an unambiguous assignment to pure d_{z2}, d_{xy}, d_{x2-y2}, d_{xz} and d_{yz} orbitals is no longer possible (see Supporting Information). Relative to **2**, the orbitals derived primarily from the d_{xy}, d_{x2-y2} and d_{z2} orbitals and predominantly d_{xz}- and d_{yz}-derived orbitals diverge in energy. Consequently, a large energy gap of ~1.5 eV separates the doubly occupied d_{z2}-like orbital from the highest-lying d-orbital hybrid. This splitting thus gives rise to the low spin $3d^7$ electronic configuration (Figure 3). In contrast, the valence isoelectronic anions $[Fe(C_9H_7)_2]^-$ and $[Fe(Cp)_2]^-$ exhibit substantially smaller separations between the corresponding orbitals of only 1.0 and 1.1 eV, respectively, therefore adopting high-spin ground states (see Supporting Information). The AILFT analysis reveals that the ligand properties of **PPI** differ fundamentally from cyclopentadienyl and indenyl, resulting in pronounced reorganization of the d-orbital manifold. This generates a large ligand-field splitting that stabilises a low-spin Fe(I) configuration. Consequently, **PPI** is particularly effective at stabilizing low-valent iron species compared to conventional metallocene ligands.

3 | Conclusion

In conclusion, we have established a synthetic route to the first ferrocene analogue featuring two biradicaloid ligands through the isolation of the Fe(I) sandwich complex **1** as a key intermediate en route to the Fe(II) complex **2**. Our investigations reveal that the **PPI** ligand profoundly influences the electronic structure of these complexes, enabling the isolation of a room-temperature-stable, low-spin Fe(I) sandwich complex, in stark contrast to the corresponding carbocyclic cyclopentadienyl analogue, which preferentially adopts a high-spin electronic configurations and is inherently unstable. These findings highlight the unique ability of biradicaloid ligands to stabilize unusual oxidation states and electronic structures in organometallic chemistry and underscore their potential as a versatile platform for the development of low-oxidation state transition-metal complexes.

Author Contributions

David Zuber: investigation, methodology, formal analysis, data curation and writing – review and editing. **Robert Kruk:** formal analysis and data curation. **Oksana Storcheva:** formal analysis and data curation. **Michael Neuwirt:** investigation, methodology and data curation. **Peter Coburger:** conceptualisation, investigation, funding acquisition, writing – original draft, writing – review and editing, formal analysis, supervision, data curation and resources. **Oliver P. E. Townrow:** conceptualisation, investigation, funding acquisition, writing – original draft, writing – review and editing, methodology, formal analysis, data curation and resources.

Acknowledgements

Financial support (VCI Liebig fellowship and YIG Prep Pro fellowship (O.P.E.T.), VCI doctoral fellowship (D.Z.), and Emmy-Noether program of the DFG (P.C., grant no 531749456)) is gratefully acknowledged. The authors further wish to acknowledge Dr. Olaf Fuhr for his assistance with SCXRD measurements and Franziska Ganslmaier for her assistance with ESI-MS measurements, access to the Karlsruhe Micro Nano Facility (KMNFi), and the state of Baden-Württemberg through bwHPC, the DFG (INST 40/575-1 FUGG) for access to the JUSTUS 2 high performance computing cluster, and the chair of Inorganic Chemistry with Focus on New Materials for access to the x-ray diffractometers. Finally, we would like to thank Prof. Stefanie Dehnen and Prof. Thomas Fässler for their continuous support and guidance.

Open access funding enabled and organized by Projekt DEAL.

Conflicts of Interest

The authors declare no conflicts of interest.

Data Availability Statement

The data that support the findings of this study are available in the Supporting Information of this article.

References

1. D. Astruc, "The Numerous Paths of Ferrocene," *Nature Chemistry* 15, no. 11 (2023): 1650–1650, https://doi.org/10.1038/s41557-023-01348-1.

2. P. L. Pauson, "Ferrocene Derivatives. Part I. The Direct Synthesis of Substituted Ferrocenes," *Journal of the American Chemical Society* 76, no. 8 (1954): 2187–2191, https://doi.org/10.1021/ja01637a046.

3. A. Straube, L. Useini, and E. Hey-Hawkins, "Multi-Ferrocene-Based Ligands: From Design to Applications," *Chemical Reviews* 125, no. 6 (2025): 3007–3058, https://doi.org/10.1021/acs.chemrev.4c00295.

4. U. Rauf, G. Shabir, S. Bukhari, F. Albericio, and A. Saeed, "Contemporary Developments in Ferrocene Chemistry: Physical, Chemical, Biological and Industrial Aspects," *Molecules* 28, no. 15 (2023): 5765, https://doi.org/10.3390/molecules28155765.

5. E. Lerayer, L. Radal, T. A. Nguyen, et al., "Highly Functionalized Ferrocenes," *European Journal of Inorganic Chemistry* 2020, no. 5 (2020): 419–445, https://doi.org/10.1002/ejic.201901183.

6. J. Fischer, A. Mitschler, L. Richard, and F. Mathey, "Phosphaferrocenes as Phosphorus Ligands. Crystal and Molecular Structure of Tetracarbonyl(3,4-Dimethylphosphaferrocene-P)Iron," *Journal of the Chemical Society, Dalton Transactions* 9 no. 12 (1980): 2522, https://doi.org/10.1039/DT9800002522.

7. E. Niecke, A. Fuchs, F. Baumeister, M. Nieger, and W. W. Schoeller, "A P_2 C_2 Four-Membered Ring With Unusual Bonding—Synthesis, Structure, and Ring Opening of a 1,3-Diphosphacyclobutane-2,4-Diyl," *Angewandte Chemie* 34, no. 5 (1995): 555–557, https://doi.org/10.1002/anie.199505551.

15213773, 0, Downloaded from https://onlinelibrary.wiley.com/doi/10.1002/anie.80193968 by Karlsruher Institut Fur Technologie, Wiley Online Library on [16/11/2026]. See the Terms and Conditions (https://onlinelibrary.wiley.com/terms-and-conditions) on Wiley Online Library for rules of use; OA articles are governed by the applicable Creative Commons License

8. D. Scheschkewitz, H. Amii, H. Gornitzka, W. W. Schoeller, D. Bourissou, and G. Bertrand, "Singlet Diradicals: From Transition States to Crystalline Compounds," *Science* 295, no. 5561 (2002): 1880–1881, https://doi.org/10.1126/science.1068167.

9. M. Sebastian, M. Nieger, D. Szieberth, L. Nyulászi, and E. Niecke, "Synthesis and Structure of a 1,3-Diphosphacyclobutadienediide: An Aniomesolytic Fragmentation of a 1,3-Diphosphetane-2,4-Diyl in Solution," *Angewandte Chemie International Edition* 43, no. 5 (2004): 637–641, https://doi.org/10.1002/anie.200352746.

10. T. Beweries, R. Kuzora, U. Rosenthal, A. Schulz, and A. Villinger, "$[P(\mu\text{-NTer})]_2$: A Biradicaloid That Is Stable at High Temperature," *Angewandte Chemie International Edition* 50, no. 38 (2011): 8974–8978, https://doi.org/10.1002/anie.201103742.

11. Z. Li, X. Chen, D. M. Andrada, et al., "$(L)_2\ C_2\ P_2$: Dicarbondiphosphide Stabilized by N-Heterocyclic Carbenes or Cyclic Diamido Carbenes," *Angewandte Chemie International Edition* 56, no. 21 (2017): 5744–5749, https://doi.org/10.1002/anie.201612247.

12. D. Rottschäfer, B. Neumann, H. Stammler, and R. S. Ghadwal, "*N*-Heterocyclic Vinylidene-Stabilized Phosphorus Biradicaloid," *Chemistry—A European Journal* 23, no. 38 (2017): 9044–9047, https://doi.org/10.1002/chem.201702433.

13. W. W. Schoeller, "The Niecke Biradicals and Their Congeners—The Journey From Stable Biradicaloids to Their Utilization for the Design of Nonlinear Optical Properties," *European Journal of Inorganic Chemistry* 2019, no. 11–12 (2019): 1495–1506, https://doi.org/10.1002/ejic.201801218.

14. J. Bresien, D. Michalik, A. Schulz, A. Villinger, and E. Zander, "Azadiphosphaindane-1,3-Diyls: A Class of Resonance-Stabilized Biradicals," *Angewandte Chemie International Edition* 60, no. 3 (2021): 1507–1512, https://doi.org/10.1002/anie.202011886.

15. E. Zander, J. Bresien, V. V. Zhivonitko, et al., "Rational Design of Persistent Phosphorus-Centered Singlet Tetraradicals and Their Use in Small-Molecule Activation," *Journal of the American Chemical Society* 145, no. 26 (2023): 14484–14497, https://doi.org/10.1021/jacs.3c03928.

16. P. Coburger, D. Zuber, C. Schweinzer, and M. Scharnhölz, "Phosphonium-Substituted Diphosphaindenylide (PPI): Exploration of Biradical Character and Ligand Properties," *Chemistry—A European Journal* 30, no. 7 (2024): e202302970, https://doi.org/10.1002/chem.202302970.

17. K. P. Lüdtke, E. Zander, F. Taube, et al., "Reaction of NHOs With Bisphosphanes—Designing Diradicaloids, Zwitterions and Radicals," *Angewandte Chemie International Edition* 64, no. 15 (2025): e202423347, https://doi.org/10.1002/anie.202423347.

18. A. Hinz, R. Kuzora, U. Rosenthal, A. Schulz, and A. Villinger, "Activation of Small Molecules by Phosphorus Biradicaloids," *Chemistry—A European Journal* 20, no. 45 (2014): 14659–14673, https://doi.org/10.1002/chem.201403964.

19. A. Hinz, A. Schulz, and A. Villinger, "On the Behaviour of Biradicaloid $[P(\mu\text{-NTer})]_2$ Towards Lewis Acids and Bases," *Chemical Communications* 52, no. 37 (2016): 6328–6331, https://doi.org/10.1039/C6CC01935H.

20. A. Schulz, "Group 15 Biradicals: Synthesis and Reactivity of Cyclobutane-1,3-Diyl and Cyclopentane-1,3-Diyl Analogues," *Dalton Transactions* 47, no. 37 (2018): 12827–12837, https://doi.org/10.1039/C8DT03038C.

21. Z. Li, Y. Hou, Y. Li, A. Hinz, and X. Chen, "Biradicaloid and Zwitterion Reactivity of Dicarbondiphosphide Stabilized With N-Heterocyclic Carbenes," *Chemistry—A European Journal* 24, no. 19 (2018): 4849–4855, https://doi.org/10.1002/chem.201705403.

22. X. Chen, L. L. Liu, S. Liu, H. Grützmacher, and Z. Li, "A Room-Temperature Stable Distonic Radical Cation," *Angewandte Chemie International Edition* 59, no. 52 (2020): 23830–23835, https://doi.org/10.1002/anie.202011677.

23. P. Coburger, F. Masero, J. Bösken, V. Mougel, and H. Grützmacher, "A Germapyramidane Switches Between 3D Cluster and 2D Cyclic Structures in Single-Electron Steps," *Angewandte Chemie International Edition* 61, no. 47 (2022): e202211749, https://doi.org/10.1002/anie.202211749.

24. J. Rosenboom, A. Villinger, A. Schulz, and J. Bresien, "Concerted Addition of Aldehydes to the Singlet Biradical $[P(\mu\text{-NTer})]_2$," *Dalton Transactions* 51, no. 35 (2022): 13479–13487, https://doi.org/10.1039/D2DT02229J.

25. D. Zuber, O. Storcheva, K. P. Lüdtke, L. Brunk, and P. Coburger, "Redox-Induced Dimerisations of a Phosphacyclic Biradicaloid," *Chemical Communications* 61, no. 13 (2025): 2798–2801, https://doi.org/10.1039/D4CC05656F.

26. Z. Li, X. Chen, L. L. Liu, M. T. Scharnhölz, and H. Grützmacher, "N-Heterocyclic Carbene Stabilized Dicarbondiphosphides: Strong Neutral Four-Membered Heterocyclic 6π-Electron Donors," *Angewandte Chemie International Edition* 59, no. 11 (2020): 4288–4293, https://doi.org/10.1002/anie.201914015.

27. M. T. Scharnhölz, P. Coburger, L. Gravogl, et al., "Bis(Imidazolium)-1,3-Diphosphete-Diide: A Building Block for FeC2P2 Complexes and Clusters," *Angewandte Chemie International Edition* no. 43 (2022): e202205371, https://doi.org/10.1002/anie.202205371.

28. S. Frei, M. Neuwirt, and P. Coburger, "Modular Design Enables Access to Onium-Substituted Diphosphacyclobutadienyl Complexes," *ChemistryEurope* 4, no. 3 (2026): e202500475, https://doi.org/10.1002/ceur.202500475.

29. D. Zuber, M. Neuwirt, and P. Coburger, "Diphosphaindenyl π-Complexes as a Platform for Hapticity-Controlled Metaloligand Design," Preprint, ChemRxiv, May 18, 2026, https://doi.org/10.26434/chemrxiv.15003502/v1.

30. L. Kink, R. Kruk, and O. P. E. Townrow, "A Simple, Air Stable Single-Ion Source of Iron(I)," *Journal of the American Chemical Society* 148, no. 15 (2026): 16255–16266, https://doi.org/10.1021/jacs.6c01660.

31. D. Zuber, M. Neuwirt, and P. Coburger, "Diphosphaindenyl π-Complexes as a Platform for Hapticity-Controlled Metaloligand Design," *Dalton Transactions* (2026), https://doi.org/10.1039/D6DT01221C, 10.1039.D6DT01221C.

32. C. Magnoux and D. P. Mills, "Metallocene Anions: From Electrochemical Curiosities to Isolable Complexes," *European Journal of Inorganic Chemistry* 2022, no. 11 (2022): e202101063, https://doi.org/10.1002/ejic.202101063.

33. M. Saito, N. Matsunaga, J. Hamada, S. Furukawa, T. Tada, and R. H. Herber, "Anionic Stannaferrocene and Its Unique Electronic State," *Chemistry Letters* 48, no. 2 (2019): 163–165, https://doi.org/10.1246/cl.180880.

34. S. M. Greer, Ö. Üngor, R. J. Beattie, et al., "Low-Spin 1,1′-Diphosphametallocenates of Chromium and Iron," *Chemical Communications* 57, no. 5 (2021): 595–598, https://doi.org/10.1039/d0cc06518h.

35. H. Song, G. Kwon, C. Citek, S. Jeon, K. Kang, and E. Lee, "Pyrrolinium-Substituted Persistent Zwitterionic Ferrocenate Derivative Enabling the Application of Ferrocene Anolyte," *ACS Applied Materials & Interfaces* 13, no. 39 (2021): 46558–46565, https://doi.org/10.1021/acsami.1c11571.

36. C. A. P. Goodwin, M. J. Giansiracusa, S. M. Greer, et al., "Isolation and Electronic Structures of Derivatized Manganocene, Ferrocene and Cobaltocene Anions," *Nature Chemistry* 13, no. 3 (2021): 243–248, https://doi.org/10.1038/s41557-020-00595-w.

37. M. Atanasov, D. Ganyushin, D. A. Pantazis, K. Sivalingam, and F. Neese, "Detailed Ab Initio First-Principles Study of the Magnetic Anisotropy in a Family of Trigonal Pyramidal Iron(II) Pyrrolide Complexes," *Inorganic Chemistry* 50, no. 16 (2011): 7460–7477, https://doi.org/10.1021/ic200196k.

38. F. Neese, F. Wennmohs, U. Becker, and C. Riplinger, "The ORCA Quantum Chemistry Program Package," *Journal of Chemical Physics* 152, no. 22 (2020): 224108, https://doi.org/10.1063/5.0004608.

39. F. Weigend and R. Ahlrichs, "Balanced Basis Sets of Split Valence, Triple Zeta Valence and Quadruple Zeta Valence Quality for H to

15213773, 0, Downloaded from https://onlinelibrary.wiley.com/doi/10.1002/anie.80193968 by Karlsruher Institut Fur Technologie, Wiley Online Library on [16/11/2026]. See the Terms and Conditions (https://onlinelibrary.wiley.com/terms-and-conditions) on Wiley Online Library for rules of use; OA articles are governed by the applicable Creative Commons License

Rn: Design and Assessment of Accuracy," *Physical Chemistry Chemical Physics* 7, no. 18 (2005): 3297, https://doi.org/10.1039/B508541A.

40. S. K. Singh, J. Eng, M. Atanasov, and F. Neese, "Covalency and Chemical Bonding in Transition Metal Complexes: An Ab Initio Based Ligand Field Perspective," *Coordination Chemistry Reviews* 344 (2017): 2–25, https://doi.org/10.1016/j.ccr.2017.03.018.

41. D. R. Blechschmidt, A. Lovstedt, and S. R. Kass, "Metallocenium Lewis Acid Catalysts for Use in Friedel–Crafts Alkylation and Diels–Alder Reactions," *Organometallics* 41, no. 18 (2022): 2648–2655, https://doi.org/10.1021/acs.organomet.2c00408.

42. A. J. Martínez-Martínez and A. S. Weller, "Solvent-Free Anhydrous Li^+ , Na^+ and K^+ Salts of $[B(3,5\text{-}(CF_3)_2C_6H_3)_4]^-$, $[BAr_4]^-$. Improved Synthesis and Solid-State Structures," *Dalton Transactions* 48, no. 11 (2019): 3551–3554, https://doi.org/10.1039/C9DT00235A.

43. O. V. Dolomanov, L. J. Bourhis, R. J. Gildea, J. A. K. Howard, and H. Puschmann, "*OLEX2*: A Complete Structure Solution, Refinement and Analysis Program," *Journal of Applied Crystallography* 42, no. 2 (2009): 339–341, https://doi.org/10.1107/S0021889808042726.

44. G. M. Sheldrick, "*SHELXT*—Integrated Space-Group and Crystal-Structure Determination," *Acta Crystallographica Section A: Foundations and Advances* 71, no. 1 (2015): 3–8, https://doi.org/10.1107/S2053273314026370.

45. G. M. Sheldrick, "Crystal Structure Refinement With *SHELXL*," *Acta Crystallographica Section C: Structural Chemistry* 71, no. Pt 1 (2015): 3–8, https://doi.org/10.1107/S2053229614024218.

46. F. Neese, "Software Update: The ORCA Program System, Version 4.0," *WIREs Computational Molecular Science* 8, no. 1 (2018): e1327, https://doi.org/10.1002/wcms.1327.

47. S. Grimme, A. Hansen, S. Ehlert, and J.-M. Mewes, "r2SCAN-3c: A "Swiss Army Knife" Composite Electronic-Structure Method," *Journal of Chemical Physics* 154, no. 6 (2021): 064103, https://doi.org/10.1063/5.0040021.

48. F. Neese, F. Wennmohs, A. Hansen, and U. Becker, "Efficient, Approximate and Parallel Hartree–Fock and Hybrid DFT Calculations. A 'Chain-of-Spheres' Algorithm for the Hartree–Fock Exchange," *Chemical Physics* 356, no. 1–3 (2009): 98–109, https://doi.org/10.1016/j.chemphys.2008.10.036.

49. R. A. Kendall and H. A. Früchtl, "The Impact of the Resolution of the Identity Approximate Integral Method on Modern Ab Initio Algorithm Development," *Theoretical Chemistry Accounts: Theory, Computation, and Modeling Theoretica Chimica Acta* 97, no. 1–4 (1997): 158–163, https://doi.org/10.1007/s002140050249.

Supporting Information

Additional supporting information can be found online in the Supporting Information section.

The authors have cited additional references within the Supporting Information [16, 38, 39, 41–49].

Supporting File 1: anie75677-sup-0001-SuppMat.zip.

Supporting File 2: anie75677-sup-0002-SuppMat.pdf.

15213773, 0, Downloaded from https://onlinelibrary.wiley.com/doi/10.1002/anie.80193368 by Karlsruher Institut Fur Technologie, Wiley Online Library on [16/11/2026]. See the Terms and Conditions (https://onlinelibrary.wiley.com/terms-and-conditions) on Wiley Online Library for rules of use; OA articles are governed by the applicable Creative Commons License